

Comparative spectroscopic studies of Cs- and K-doped polyacetylene

S. Chiali* and P. Bernier

Groupe de Dynamique des Phases Condensées, Université de Montpellier II, Place E. Bataillon, 34095 Montpellier Cédex 05, France

S. Lefrant

Laboratoire de Physique Cristalline, Institut des Matériaux, 2 rue de la Houssinière, 44072 Nantes Cédex 03, France

R. Nuffer

Institut Charles Sadron, 6 rue Boussingault, 66083 Strasbourg Cédex, France

(Received 17 January 1995)

In this paper, we report combined NMR and resonance-Raman-scattering (RRS) results on $(\text{CH})_x$ doped with Cs at different dopant concentrations. With ^{133}Cs NMR, a resonance line is shifted at ≈ 30 ppm at low concentration ($\approx 5\%$) attributed to a diluted phase, whereas a second line at ≈ -300 ppm is recorded for higher concentrations, attributed to an ordered stage-1 phase. With RRS, usual results are obtained until a concentration level $y=8\%$, with the observation of two doping-induced Raman-active vibrational modes at 1272 and 1576 cm^{-1} . For higher concentrations ($y=9.5\%$), an additional doping-induced Raman mode is recorded at ≈ 1518 cm^{-1} . These features are in total agreement with the NMR results, provided distinct perturbations, corresponding to the two phases, are taken into account to explain Raman data. These features in the case of Cs-doped $(\text{CH})_x$, differ significantly from previous results obtained in highly n -doped systems like $(\text{CHK}_y)_x$.

I. INTRODUCTION

Intercalated compounds have been extensively studied in the past and continue to attract interest from scientists, due also to the discovery of new systems like fullerenes. In this field, conducting polymers have played a major role because many different structures have been found depending on parameters such as the nature of the intercalant ("dopant") and the doping level. This is particularly true for polyacetylene, as recalled in Ref. 1, where an incommensurate two-dimensional (2D) triangular superlattice of channels is found in Na-doped $(\text{CH})_x$ at a concentration level of 6–10% (Ref. 2), or a centered 2D square superlattice (K doping), or even a 3D long-range order sublattice for K, Rb, or Cs doping in highly oriented samples. Most of the studies were carried out on electrochemically doped polymers because this method allows at the same time to establish a clear correlation with intercalation stages. This is not straightforward, however, for large-size intercalants like Rb or Cs for which the doping procedure turns out to be rather difficult, as described earlier³ for electrochemical Cs doping of $(\text{CH})_x$. The vapor-phase technique is another way of doping, which is commonly used in the case of alkali metals for a number of different purposes including structural studies. As an example, the x-ray structure of $(\text{CH})_x$ doped with Cs at saturation using this procedure has been recently presented.¹ Nevertheless, this method of doping presents the disadvantage of leading to significantly inhomogeneous samples, especially at intermediate doping levels. A way to avoid this difficulty is to perform a chemical doping for which the doping level is thermodynamically controlled by using organic compounds with various redox potentials. The method has been described in details elsewhere^{4,5} and has proved to

be successful for quite a large number of dopants. In particular, it has been used to prepare homogeneous Cs-doped $(\text{CH})_x$ at different dopant concentrations to carry out the spectroscopic studies presented here.

The purpose of this paper is, therefore, to describe peculiar results observed in Cs-doped $(\text{CH})_x$ by using two different spectroscopic techniques such as solid-state NMR and resonance Raman scattering (RRS), for which a clear correlation can be made between the experimental data obtained with the two techniques. An interpretation of the results is then proposed in the framework of the perturbation method used to explain experimental Raman data used in n -doped systems as published recently.⁶

II. EXPERIMENTAL RESULTS

A. Sample preparation

Polyacetylene films, with a thickness of about 700–800 μm were synthesized using a modified Shirakawa technique as previously reported.⁷ Small pieces were cut from these films and n doped by immersion in various organoalkali salts in tetrahydrofuran (THF). As already mentioned, homogeneous samples were obtained since the doping level was thermodynamically controlled by using organic compounds with various redox potentials and numerous dopant concentrations were achieved for NMR studies. In this paper we present only three different levels, which we found characteristic of our study, i.e., 5, 8.1, and 9.5% using the radical ion of acenaphthylene, benzophenone, and the dianion of the 1,1-diphenylethylene, respectively.

^{133}Cs NMR spectra were recorded at room temperature with a BRUKER CXP200 spectrometer operating at

26.2 MHz. Raman spectra were obtained also at room temperature, directly in the NMR tube. We used a Jobin-Yvon HG2S as the double monochromator equipped with holographic gratings and terminated with a cooled AsGa photomultiplier as a detector. Excitation lines were provided by either an argon ion or a krypton ion laser (Spectra Physics 170).

B. Spectroscopic results

1. NMR Results

The ^{133}Cs NMR spectra obtained for the three different samples [Cs-doped $(\text{CH})_x$ at 5, 8.1, and 9.5%] are presented in Fig. 1. The spectrum shown in Fig. 1(a) shows a unique resonance only slightly shifted (≈ 30 ppm) from the reference position (Cs^+ in CsNO_3 aqueous solution). Figures 1(b) and 1(c) show an additional resonance line at ≈ -300 ppm. As it can be observed, this new line is not affected in position by the dopant concentration, but its intensity and width increase with the doping level y . At the same time, the intensity of the line peaked at about 30 ppm decreases with increasing y . Notice that this tendency is further observed in a sample doped with Cs at $\approx 16\%$ (not shown here): the peak at 30 ppm almost totally disappears.⁸

2. RRS Results

We present in Fig. 2 the RRS spectra recorded with $\lambda_{\text{exc}} = 514.5$ nm at room temperature on the three samples studied in NMR, i.e., doped with Cs at a concentra-

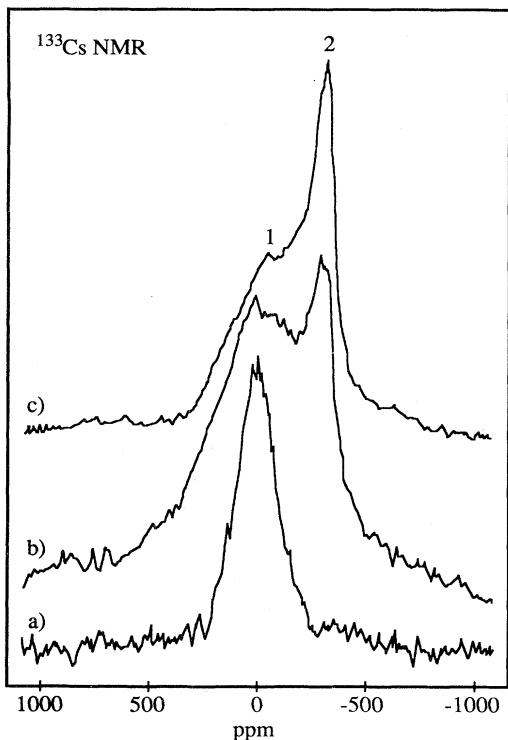


FIG. 1. RMN spectra of $(\text{CHCs}_y)_x$. (a) $y = 5\%$; (b) $y = 8.1\%$; (c) $y = 9.5\%$.

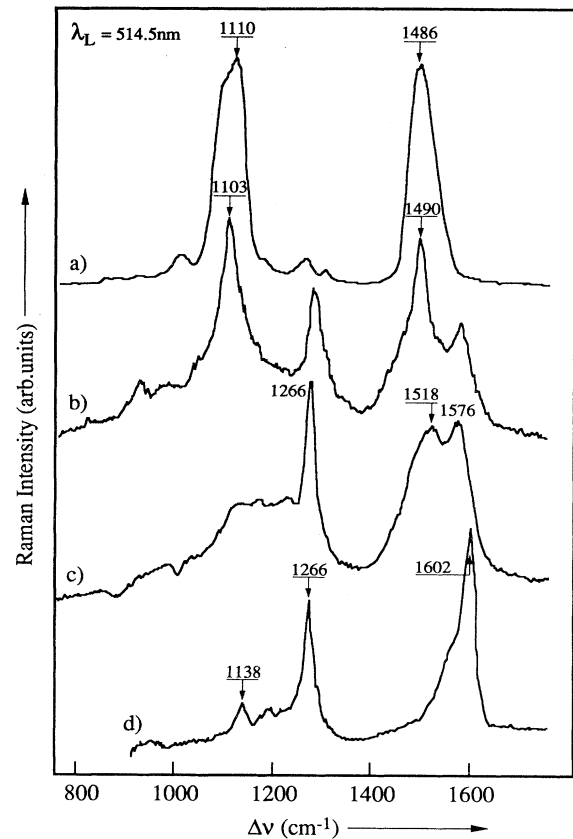


FIG. 2. RRS spectra of $(\text{CHM}_y)_x$ taken at RT with $\lambda_{\text{exc}} = 514.5$ nm. (a) $M = \text{Cs}$, $y = 5\%$; (b) $M = \text{Cs}$, $y = 8.1\%$; (c) $M = \text{Cs}$, $y = 9.5\%$; (d) $M = \text{K}$, $y = 15-16\%$.

tion level of 5, 8.1, and 9.5%, respectively. For comparison, we have also indicated in Fig. 2(d), the RRS spectrum of $(\text{CH})_x$ doped with K at saturation. The Raman spectrum of $(\text{CHCs}_{0.05})_x$ [Fig. 2(a)] is composed of two main bands at ≈ 1110 and 1486 cm^{-1} , which, in addition, exhibit shoulders on their low-frequency side. Figure 2(b) shows the RRS spectrum of $(\text{CHCs}_{0.081})_x$, which is drastically modified since the Raman bands observed before are much more narrow and slightly shifted to 1103 and 1490 cm^{-1} , respectively. Moreover, two additional bands are recorded at 1272 and 1576 cm^{-1} .

For $(\text{CHCs}_{0.095})_x$, the RRS spectrum is again totally different. The two additional peaks reported in the previous case are still observed (at 1266 and 1576 cm^{-1}), but the two bands at 1103 and 1490 cm^{-1} are no longer present in the spectrum. In addition, a new broad Raman band is recorded at ≈ 1518 cm^{-1} together with weak features in the frequency range 1100–1250 cm^{-1} . Finally, the RRS spectrum of $(\text{CHK}_{0.15})_x$ shown in Fig. 2(d) is mainly composed of Raman bands as 1266 and 1590 cm^{-1} as usually observed in n -doped $(\text{CH})_x$ at saturation and reported previously.⁶

III. DISCUSSION AND CONCLUSION

From the NMR spectra presented in Sec. II, the two resonance lines strongly suggest the presence of two

different phases for lightly doped $(\text{CHCs}_y)_x$. First of all, the line observed at ≈ 30 ppm in highly doped samples is attributed to purely ionic Cs dopants, randomly distributed in the polymer. By comparison with results obtained on $(\text{CHK}_y)_x$, it would correspond to a stage-2 diluted phase. As a matter of fact, a stage-2 phase has already been put in evidence by x-ray diffraction by Saldi *et al.*,⁹ who proposed a channel structure with a rectangular cell. Then, as long as the dopant concentration increases, this phase deorganizes to the benefit of a new ordered one where Cs^+ dopants are arranged in a regular manner within the polymer. That would correspond to a stage-1 phase. This assignment is confirmed from x-ray results obtained from a $(\text{CH})_x$ doped with Cs at saturation in which such an ordered stage is observed.¹

The Raman features may be analyzed in complete consistency with these results. As it is well known, the resonance-Raman-scattering spectroscopy has been widely used to investigate $(\text{CH})_x$ in both pristine and doped states. Different theories have been elaborated and among them, the model which describes the polymer in terms of a double distribution of conjugated segments (for details, see Ref. 10). In the case of doped samples, RRS spectra have shown drastic modifications in the case of p dopants, but especially in the case of n dopants as reported by several groups.^{11–17} In particular, for dopant concentrations higher than 6%, additional Raman appear in the spectra at 1270 and ≈ 1600 cm^{-1} . These maxima depend on the excitation wavelength. This is exactly what is observed in the Cs-doped $(\text{CH})_x$ for concentration levels such as $y=5$ and 8.1%, respectively. A complete analysis of the Raman spectra of n -doped $(\text{CH})_x$, including the isotope derivatives $(^{13}\text{CH})_x$ and $(\text{CD})_x$ has been published recently⁶ for K doping at different concentrations.

The RRS experimental results presented are rather well understood if one uses the theoretical model developed to explain the features of doping-induced and photoinduced infrared spectra in $(\text{CH})_x$ (Refs. 10, 18, and 19). This model includes calculations of the perturbed lattice dynamics of the conjugated segments by using the perturbed-Green function formalism. The perturbation, which is induced by the trapped charges on the lattice dynamics of the conjugated segments, is taken into account by a parameter Λ . In the frame of this formalism, the density of perturbed vibrational states $\rho(\omega^2)$ can be written in terms of Λ , $\tilde{\rho}^0(\omega^2)$ and $\rho^0(\omega^2)$, which are the real and imaginary parts, respectively, of the unperturbed Green function $G^0(\omega^2+i0^+)\rho(\omega^2)$ can be expressed as follows:

$$\rho(\omega^2) = \frac{\rho^0(\omega^2)}{[1 - \tilde{\rho}^0(\omega^2)\Lambda]^2 + [\pi\rho^0(\omega^2)\Lambda]^2}$$

$\tilde{\rho}^0(\omega^2)$ as a function of ω is presented in Fig. 3 for $\text{trans}(\text{CH})_x$ (from Ref. 6). In this theory, only localized modes due to the perturbation can be evaluated, whose frequencies are deduced in solving the equation

$$\frac{1}{\Lambda} = \tilde{\rho}^0(\omega^2)$$

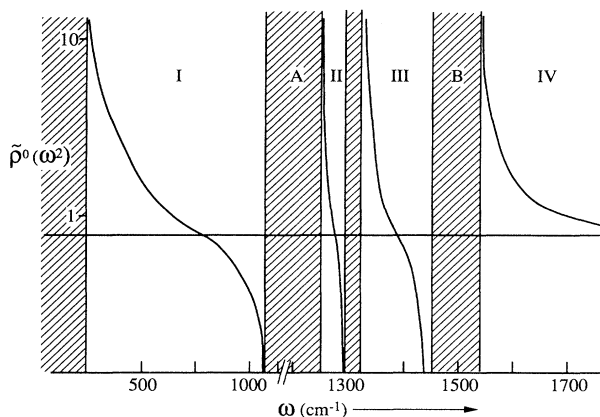


FIG. 3. Calculated $\tilde{\rho}^0(\omega^2)$ as a function of ω in $\text{trans}(\text{CH})_x$. Values are given in $10^{-7}/\text{cm}^2$. For explanation, see Ref. 6.

As shown in Ref. 6, the doping-induced Raman-active vibrational modes are found in region II and IV, considering a positive change of Λ . Therefore, one can deduce the value of Λ which leads to the 1270 and the ≈ 1600 cm^{-1} Raman modes observed experimentally [Figs. 2(d) and 2(b)]. In the case of $(\text{CHK}_{0.15})_x$, the perturbation parameter Λ was evaluated to be in the range $1.5-4 \times 10^6$ cm^{-1} (modes at 1540–1600 and 1265–1275 cm^{-1} in $(\text{CHK}_{0.15})_x$ depending on the laser wavelength). If one compares to the $(\text{CHCs}_{0.081})_x$ case, it accounts well for the 1275 and 1576 cm^{-1} doping-induced Raman modes observed with $\lambda_{\text{exc}}=514.5$ cm^{-1} . Note that in addition, the spectrum [Fig. 2(b)] exhibit characteristic of short undoped segments (Raman bands at 1103 and 1490 cm^{-1}), in agreement with a rather dilute phase as described to explain NMR results. Notice also that these two bands have rather strong “tails” whose origin can be different.

In the case of $(\text{CHCs}_{0.095})_x$, strong modifications are observed in the spectrum [Fig. 2(c)]. Raman bands due to undoped conjugated segments are no longer observed and a new strong and broad band peaked at ≈ 1518 cm^{-1} is recorded. This spectrum is also significantly different with the one recorded for $(\text{CHK}_{0.15})_x$. If one considers the behavior of $\tilde{\rho}^0(\omega^2)$ shown in Fig. 3, one can deduce from the slopes of the curves drawn in regions II and IV that changing Λ (which can be represented by an horizontal line) changes considerably the frequency of the doping-induced Raman mode in region IV, whereas it will almost not affect the one in region II. Therefore, the appearance of a new doping-induced Raman mode in spectrum 2c [Fig. 2(c)] is interpreted as a new perturbed phase, whose perturbation is much larger than in the previous case. On the other hand, this perturbation induces a second Raman-induced mode at a frequency close to the one peaked before, the contribution of both leading to the 1266 cm^{-1} line. Following this interpretation, one may then consider that in $(\text{CHCs}_{0.095})_x$, two perturbed phases coexist for this dopant level. The less perturbed one would correspond to the ordered stage-1 phase, both being suggested from NMR results. Let us mention finally that the case $(\text{CHCs}_{0.095})_x$ is unique since it has never

been observed in other *n*-doped systems, even at higher concentration levels. The presence of two doping-induced Raman bands in the region 1400–1600 cm^{-1} seems to be specific to Cs-doped $(\text{CH})_x$ highly oriented and highly doped with Cs in the vapor phase. Any interpretation involving 3D effects in oriented samples can be ruled out because our samples were not oriented.

In conclusion, we have reported NMR and RRS results on $(\text{CH})_x$ doped chemically with Cs, which ensures a good homogeneity. For the first time in *n*-doped systems, experimental data seem to reflect two different phases in samples doped at concentration levels higher than 9%.

This is put in evidence by two distinct resonance lines in NMR, whereas two different sets of doping-induced Raman vibrational modes are observed, presumably due to two distinct perturbations induced by the presence of

Cs^+ ions close to the polymer backbone. These results are significantly different from what was previously observed even at high concentrations in *n*-doped $(\text{CH})_x$ systems.⁶ Further experiments would be needed in order to check if these results are correlated with the dopant size, by investigating systems like $(\text{CHRb}_y)_x$ for example.

ACKNOWLEDGMENTS

This work was partly supported by the European Contract Brite-Euram "HICOPOL". The Groupe de Dynamiques des Phases Condensées is "Unité de Recherche Associée" au CNRS No. 233. The Institut des Matériaux is "Unité Mixte de Recherche" CNRS/Université de Nantes No. 110. The Institut Charles Sadron is "Unité Propre de Recherche" CNRS No. 22.

*Present address: Institut de Physique, Université d'Oran Es-Senia, Oran, Algeria.

- ¹J. Ma, D. Djurado, J. E. Fischer, N. Coustel, and P. Bernier, *Phys. Rev. B* **41**, 2971 (1990).
- ²M. J. Winokur, Y. B. Moon, A. J. Heeger, J. Baker, D. C. Bott, and H. Shirakawa, *Phys. Rev. Lett.* **58**, 2329 (1987).
- ³M. Zagorska, P. Bernier, M. Armand, and J. L. Sauvajol, *Synth. Met.* **41-43**, 3093 (1991).
- ⁴B. François, C. Mathis, R. Nuffer, and A. Rudatsikira, *Mol. Cryst. Liq. Cryst.* **117**, 113 (1985).
- ⁵C. Mathis, A. Rudatsikira, R. Nuffer, and B. François, *Makromol. Chem. Makromol. Symp.* **24**, 99 (1989).
- ⁶S. Lefrant, E. Mulazzi, and C. Mathis, *Phys. Rev. B* **49**, 13 400 (1994).
- ⁷B. François, M. Bernard, and J. J. André, *J. Chem. Phys.* **75**, 4142 (1981).
- ⁸S. Chiali, thèse d'Etat, Université d'Oran es-Senia 1993.
- ⁹F. Saldi, J. Ghanbaja, D. Begin, M. Lelaurain, and D. Billaud, *C. R. Acad. Sci.* **309**, 671 (1989).
- ¹⁰G. P. Brivio and E. Mulazzi, *Phys. Rev. B* **30**, 876 (1984).
- ¹¹E. Faulques and S. Lefrant, *J. Phys. (Paris) Colloq.* **44**, C3-337 (1983).
- ¹²I. Harada, Y. Furukawa, M. Tasumi, H. Shirakawa, and S. Ikeda, *J. Chem. Phys.* **73**, 4776 (1980).
- ¹³E. Faulques, S. Lefrant, F. Rachdi, and P. Bernier, *Synth. Met.* **9**, 53 (1984).
- ¹⁴S. Lefrant, E. Faulques, A. Chentli, F. Rachdi, and P. Bernier, *Synth. Met.* **17**, 313 (1987).
- ¹⁵H. Eckhard, L. W. Shacklette, J. S. Szobota, and R. H. Baughman, *Mol. Cryst. Liq. Cryst.* **117**, 401 (1985).
- ¹⁶J. Tanaka, Y. Saito, H. Shimizu, C. Tanaka, and M. Tanaka, *Bull. Chem. Soc. Jpn.* **60**, 1595 (1987).
- ¹⁷J. Tanaka, Y. Saito, H. Shimizu, and M. Tanaka, *Synth. Met.* **17**, 307 (1987).
- ¹⁸E. Mulazzi, A. Ripamonti, T. Verdon, and S. Lefrant, *Phys. Rev. B* **45**, 9439 (1992).
- ¹⁹E. Mulazzi, A. Ripamonti, and S. Lefrant, *Solid State Commun.* **83**, 821 (1992).